Correspondence between resting state activity and brain gene expression

Guang-Zhong Wang[1,10], T. Grant Belgard[2,10,12], Deng Mao[3,13], Leslie Chen[5], Stefano Berto[1], Todd M. Preuss[6], Hanzhang Lu[3,4,13], Daniel H. Geschwind[2,5,7,8,9,11] & Genevieve Konopka[1,11].

Affiliations:

[1]Department of Neuroscience, The University of Texas Southwestern Medical Center, Dallas, TX 75390, USA.
[2]Program in Neurobehavioral Genetics, Semel Institute, David Geffen School of Medicine, University of California, Los Angeles, Los Angeles, CA 90095, USA.
[3]Advanced Imaging Research Center, [4]Departments of Psychiatry and Radiology, The University of Texas Southwestern Medical Center, Dallas, TX 75390, USA
[5]Interdepartmental Program in Neuroscience, University of California, Los Angeles, Los Angeles, CA 90095, USA
[6]Division of Neuropharmacology and Neurologic Diseases, Yerkes National Primate Research Center, Emory University, and Department of Pathology, Emory University School of Medicine, Atlanta, GA 30329, USA
[7]Department of Human Genetics, David Geffen School of Medicine, University of California, Los Angeles, Los Angeles, CA 90095, USA
[8]Center for Autism Treatment and Research, Semel Institute, David Geffen School of Medicine, University of California, Los Angeles, Los Angeles, CA 90095, USA
[9]Program in Neurogenetics, Department of Neurology, David Geffen School of Medicine, University of California, Los Angeles, Los Angeles, CA 90095, USA
[10]These authors contributed equally to this work.
[12]Current address: MRC Functional Genomics Unit, Department of Physiology, Anatomy and Genetics, University of Oxford, South Parks Road, Oxford OX1 3PT, UK.
[13]Current address: The Russell H. Morgan Department of Radiology & Radiological Science, Johns Hopkins University School of Medicine, Baltimore, MD 21287, USA
[11]Correspondence to: dhg@ucla.edu; genevieve.konopka@utsouthwestern.edu.

The relationship between functional brain activity and gene expression has not been fully explored in the human brain. Here, we identify significant correlations between gene expression in the brain and functional activity by comparing fractional Amplitude of Low Frequency Fluctuations (fALFF) from two independent human fMRI resting state datasets to regional cortical gene expression data from a newly generated RNA-seq dataset and two independent

gene expression datasets to obtain robust and reproducible correlations. We identify functional pathways correlated with brain activity. We find significantly more genes correlated with fALFF than expected by chance, and identify specific genes correlated with the imaging signals in multiple expression datasets in the default mode network. Together, these data support a population-level relationship between regional steady state brain gene expression and resting state brain activity.

Understanding the molecular underpinnings of complex human brain circuits requires integration of multiple forms of high-dimensional data, ranging from functional brain imaging[1, 2] to genetic and genomic analyses. Seminal work in neuroimaging over the last decade has revealed that human brain activity can be defined by its network properties[3-6]. Differences in gene regulation and expression have also been related to brain function in many species[7-9] and to the evolution of human higher cognitive functions[10-15]. Here, we link these diverse levels of analysis by asking whether gene expression in human neocortex is correlated to functional networks defined by fMRI in humans (**Fig. 1a**).

RESULTS

Functional correlation between gene expression and fMRI signals

To assess the relationship between gene-expression regulation and human brain activity, we generated a human neocortical RNA-sequencing (RNA-seq) dataset and

compared it to resting state fMRI data[16]. We carried out RNA-seq of ~50 adult human postmortem neocortical brain samples representing 10 neocortical brain regions: pre-motor cortex (PMV; BA6 (Brodmann Area 6)), dorsolateral prefrontal cortex (DLPFC; BA9), posterior middle temporal gyrus (pMTG; BA21), posterior superior temporal gyrus (pSTG; BA22), angular gyrus (AG; BA39), supramarginal gyrus (SMG; BA40), pars opercularis (POP; BA44), pars triangularis (PTr; BA45), middle frontal gyrus (MFG; BA46), and pars orbitalis (POrB; BA47). For each brain region, three or more samples from left adult brain hemispheres were collected (ages range from 33 to 49) (**Supplementary Tables 1** and **2**). An example of the gene expression profiles across our RNA-seq samples is illustrated in **Supplementary Figure. 1**.

For the resting state fMRI data, we measured the spontaneous fluctuations of brain activity in each neocortical region by calculating the fractional Amplitude of Low Frequency Fluctuations (fALFF, the fraction of amplitude in the 0.01 – 0.08 Hz frequency range)[17], which is considered a proxy for regional brain activity, from a large publicly available fMRI dataset (fMRI_1) (**Supplementary Tables 3** and **4**)[16]. The average fALFF values of all individuals were used as the baseline functional feature of the brain region to measure correlations of gene expression with fALFF values using three gene expression datasets. We generated our own RNA-seq samples from 10 neocortical brain regions, and assessed these findings using samples from ages five and older from two additional large scale datasets: RNA-seq data from Brainspan (www.brainspan.org) and microarray data from Kang et al.[18], which each consist of 11 neocortical brain regions (**Fig. 1b**). We also replicated the three sets of calculations in

an independent resting state fMRI dataset (fMRI_2) (**Fig. 1b**). Only genes whose correlations replicated (Fisher r-to-z transformation, two-tailed $P < 0.005$) in at least one dataset besides the discovery dataset were included for further analysis. In addition, we did not find a significant effect of sex on correlations between gene expression and fMRI activity (**Supplementary Fig. 2**).

To determine whether correlations between gene expression and fMRI are due to specific brain functions, we carried out gene ontology (GO) analyses. We identified 20 functional categories whose genes were consistently correlated, positively or negatively, with fALFF (**Fig. 1b** and **Supplementary Table 5**), and replicated in both fMRI datasets. In the fMRI_1 dataset, most of the GO terms that had a globally significant bias towards being positively or negatively correlated with fALFF in one gene expression dataset had a globally significant bias in the opposite direction in another gene expression dataset. However, all terms were consistent in the fMRI_2 dataset. These data highlight the need for ascertaining more complete GO annotations for brain expressed genes. Three of these consistent functions are particularly interesting in terms of their potential role in regulating overall brain activity: G-protein coupled receptor (GPCR), signaling receptor and synaptic membrane genes are more likely to be negatively correlated with fALFF. These functions are important for proper signal transduction in neural circuits. For example, many neurotransmitter receptors are G-protein coupled and the synaptic membrane plays a complex role in propagating upstream signals to the next neuron in the circuit. GPCRs are highly enriched in the brain, and the majority of drugs available for treating brain disorders target GPCRs[19]. The negative correlation of these functional

categories to resting state fALFF is surprising and could be indicative of either negative feedback regulation of frequently utilized neuronal connections during the resting state or refinement of synaptic density to efficiently mediate neurotransmission during the resting state. Thus, while the enrichment of these functional categories to cortical brain gene expression suggests that these pathways are involved in mediating resting state brain function, such correlations should be investigated in future studies.

Individual genes correlate with fMRI signals

We then identified the individual genes that show consistent correlation patterns across the gene expression and fMRI datasets by narrowing the brain regions analyzed to those involved in the default mode network (DMN). This comparison should be more physiologically meaningful when using resting state imaging data, as much of the brain activity during a wakeful resting state may be limited such networks[20, 21]. First, we computed whether gene expression is globally more likely to correlate with fALFF than expected by chance. By permuting fALFF assignments to brain regions, we find that the number of observed fALFF correlated genes is significantly higher than expected in each of the three datasets (empirical P = 0.04 for our RNA-seq, P = 0.004 for Kang et al. and P = 0.03 for Brainspan, **Fig. 2a-c**). We defined fALFF-correlated genes as those genes that have significant correlations in at least two out of three datasets (**Fig. 1b**, Fisher r-to-z transformation, two-tailed $P < 0.005$) for both fMRI datasets. We identified 38 correlated genes using these criteria (**Supplementary Table 6**). All of these 38 genes are correlated in the same direction in both fMRI datasets, with 12 of them

positively correlated and 26 of them negatively correlated with fALFF. We find that the correlation levels of these genes are highly similar in the two fMRI datasets (Pearson correlation coefficient r > 0.99 on average, **Fig. 3**), indicating the robustness of this analysis across imaging cohorts. Remarkably, the expression pattern of 26 of the 38 genes can each explain 10% or more of the statistical variance in fALFF (**Table 1**).

Gene ontology analysis of these fALFF-correlated genes identified significant enrichment of the cellular categories endoplasmic reticulum and mitochondrion. The small number and general nature of the categories are most likely due to the relatively small number of genes that are correlated and available for GO analysis (38). However, a number of these genes are quite interesting in terms of brain function and disease. In **Figure 4a**, we illustrate a few of the most highly positive and negatively correlated genes. Remarkably, many of these genes have previously been implicated in neuronal activity or dysfunction, suggesting an important function for these genes in resting state activity that is disrupted in cognitive diseases. *SYT2* encodes an integral membrane protein of synapses and can increase the dynamic range of synapses by maximizing calcium-evoked neurotransmitter release[22]. *SCN1B*, which regulates the Na+ current in neurons, has been implicated in epilepsy and Dravet syndrome[23-26]. *GLRA2* is a ligand-gated ion channel that is widely expressed in the central nervous system and plays an important role in the inhibition of neuronal firing[27]. *DRD2* as well as *HAPLN4* (see **Supplementary Table 6**) were recently identified in the largest schizophrenia GWAS to date as two of the genes near the highly associated loci[28].

fALFF-correlated genes have greater expression in neurons

Based on these clear links between the most highly correlated genes and neuronal function, we examined a genome-wide database of brain cell type specificity[29]. For all genes with available cell-type expression data, we determined the cellular preference of expression for each gene based on the highest RPKM value among the seven defined cell types. We find that many (14) of the highly fALFF-correlated genes are preferentially expressed in neurons (**Supplementary Fig. 3** and **Supplementary Table 7**, P = 0.003; Fisher's exact test) and >85% (12 out of the 14 genes with preferential neuronal expression) of these genes have at least two times higher expression in neurons compared to the maximum expression of other cell types. Interestingly, only two genes have the greatest expression in endothelial cells, *TNNT1* and *GPD2* (**Supplementary Table 7**). These results suggest that the correlation between fMRI and gene expression is not likely driven by dynamic range as a function of vascular density, but rather by a signature derived from neuronal function. Such a finding might be expected given that fALFF has been reported to be sensitive specifically to detecting neuronal activity[17].

fALFF-correlated genes are correlated to ASD coexpression modules

Since we conducted focused comparisons using only DMN brain regions and previous work has shown that the DMN is disrupted in cognitive disorders such as autism spectrum disorders (ASD)[30], we examined whether salient ASD brain gene expression

patterns overlap with the highly fALFF-correlated genes. We find 9 fALFF-correlated genes that are contained within the autism gene co-expression module, asdM12, a set of genes downregulated in autism previously identified from postmortem ASD brain tissue (**Supplementary Table 8**, *P* = 8e-5; Fisher's exact test)[31]. Only one of these genes is not positively correlated with resting state fALFF (**Supplementary Table 8).** By definition, the genes within the asdM12 module are highly co-expressed with one another. We therefore computed the expression correlations of the 38 fALFF-correlated genes. By permuting pairs of genes, we find that the fALFF-correlated genes show approximately 2 fold higher co-expression than other genes (*P* < 1e-3) and there is no bias towards positive or negative correlations (**Fig. 4a**, **Supplementary Fig. 4** and **5**). As the genes in the asdM12 module are enriched with neuronal and synaptic markers and tend to be downregulated in autism brains[31], our results again highlight the importance of these correlated genes in normal brain function.

fALFF-correlated genes are enriched in brain regional DE genes

Previous human brain transcriptome studies have noted a dearth of genes differentially expressed (DE) between cortical areas[32, 33], and much of the differential expression driving cortical diversity likely derives from laminar specificity. However, there has been very little functional characterization of these cortical DE genes or ideas put forth as to how their expression pattern may contribute to overall brain function. Based on our method of calculating correlations between fALFF and gene expression, we have identified differential gene expression signatures between cortical areas that correspond

to the differential brain activity. To confirm this, we assessed pair-wise brain regional differential expression in either all 10 brain regions sequenced or only the DMN regions (**Supplementary Tables 9** and **10**). We identified 1,083 DE genes across all regions and 545 DE genes across only the DMN regions. We find that 78% of the identified fALFF-correlated genes are indeed differentially expressed (DE) genes (30/38, P = 6e-28). Twenty of the fALFF-correlated genes are also differentially expressed during neocortical developmental (**Supplementary Table 6**)[32]. We find that the DE genes have significantly higher correlations with fALFF than non-DE genes, regardless of whether the DE derives from using 10 brain regions or the DMN regions (**Supplementary Fig. 6a**,**b**, P < 1e-10 in all the comparisons). More importantly, regardless of whether the DE genes derive from all brain regions or only the DMN regions these genes are more likely correlated with fALFF signals than expected (**Fig. 4b,c**, P < 0.05). Together, these results are consistent with a functional role of these regional DE genes in steady state brain activity. A recent study has also found correlation between cortical gene expression and two functionally defined brain networks. In contrast to our study, this other study finds that two of our top positively correlated genes with the DMN, *SCN1B* and *SYT2*, are correlated with what these authors define as a functional visual-sensorimotor-auditory network[34]. Therefore, while the other study did not use fMRI values correlated to gene expression as we have done, these findings complement our work by identifying some of the same genes corresponding to known functionally connected networks based on brain imaging.

DISCUSSION

To the best of our knowledge, this is the first study to directly correlate the transcriptome to measurements of human brain activity. Here, we correlate RPKM, a measurement of steady state gene expression with fALFF, a measurement for resting state activity within a single brain region. Therefore, in contrast to functional connectivity approaches, the use of fALFF allows for direct measurement of the amplitude of brain activity within a single brain region, rather than between region correlations[17]. A limitation of this study is that we cannot directly address whether resting state brain activity influences gene expression or *vice versa* given the use of post-mortem brain tissue for expression. However, the identification of these genes whose expression is related to brain networks opens the possibility of exploring such directional functional relationships between gene expression and brain activity in animal models. Moreover, due to limited availability of additional brain tissue from independent studies for gene expression that correspond to additional DMN regions, future studies will need to explore the robustness of our results throughout the DMN and other resting state networks. However, as the regions of interest among gene expression studies in fact capture different parts of the DMN (**Supplementary Tables 3** and **4**), we expect some overlap in gene correlations in additional areas. Finally, this study provides a framework for future investigations into cognitive disorders with altered DMN function such as ASD. The future identification of correlations between fMRI and gene expression in ASD brains will determine whether the correlated genes we identified in this study have altered patterns in a disease state.

Materials and Methods

Sample Information

Post-mortem tissue from ten neocortical brain regions from adult males was used in this study. These regions are pre-motor cortex (PMV; BA6 (Brodmann Area 6)), dorsolateral prefrontal cortex (DLPFC; BA9), posterior middle temporal gyrus (pMTG; BA21), posterior superior temporal gyrus (pSTG; BA22), angular gyrus (AG; BA39), supramarginal gyrus (SMG; BA40), pars opercularis (POP; BA44), pars triangularis (PTr; BA45), middle frontal gyrus (MFG; BA46), and pars orbitalis (POrB; BA47). Detailed sample information is included in **Supplementary Table 1**.

Sample preparation and RNA sequencing

Frozen tissue samples from human post-mortem brains were used. Samples were dissected from frozen tissue pieces provided by the Maryland Brain and Tissue Bank. Total RNA was extracted using QIAGEN miRNeasy kits according to the manufacturer's instructions. All RNA samples were examined for quantity and quality by NanoDrop and Bioanalyzer (Agilent). RINs (RNA integrity numbers) are included in **Supplementary Table 1**. 1 µg of total RNA from each sample was used, and samples were randomized for RNA extractions and sequencing. Libraries were prepared using an Illumina TruSeq kit according to the manufacturer's instructions. Samples were barcoded and 3 barcoded samples were run per lane on an Illumina HiSeq according to the manufacturer's instructions. Single-end 100bp reads were aligned in a staged manner. First, reads were aligned with tophat2 using default options to a reference sequence

comprised of mitochondrial DNA, mitochondrial cDNA, and ribosomal cDNA (GRCh37, Ensembl release 67). These reads were excluded from further analysis. The reads that did not map in the first iterations were then mapped using tophat2 to GRCh37 using the GTF provided in Ensembl release 67. RPKMs were then quantified using cufflinks, providing gene definitions (Ensembl release 67 GTF), and enabling several options (fragment bias correction, multi-read correction, upper quartile normalization, and compatible hits normalization). Gene-level RPKM quantifications were used for all downstream processing. Scaled by multiplying the appropriate factor to set each 80th percentile RPKM to be the geometric mean 80th percentile RPKM among samples. The NCBI Gene Expression Omnibus (GEO) accession number for the RNA-seq data reported in this manuscript is GSE58604. Reviewers can access through this link: http://www.ncbi.nlm.nih.gov/geo/query/acc.cgi?token=ozgnkucodnujdqt&acc=GSE58604. Since correlative measures are highly sensitive to zero values, we used the 17,469 genes that were expressed at a nonzero level in each sample. We repeated analyses with and without outlier removal and found it had no substantial impact on the results with these data.

fMRI data processing and analysis

The fMRI data were downloaded from The 1000 Functional Connectomes Project[16] (http://www.nitrc.org/frs/?group_id=296, Cambridge_Buckner dataset (fMRI_1) and New York dataset (fMRI_2)). fMRI_1 measures the time series resting state signal of 198 adult individuals and fMRI_2 measures 84 individuals. Both datasets were acquired using gradient-echo echo-planar-imaging on 3 Tesla scanners. For Cambridge_Buckner

dataset, 119 volumes were acquired under the following parameters: TR = 3000 ms, voxel size = 3 × 3× 3 mm^3, FOV = 216 × 216 mm^2, 47 slices, TE = 30 ms, flip angle = 85 degrees; For New_York dataset, 192 volumes were acquired under the following parameters: TR = 2000 ms, voxel size = 3 × 3× 3 mm^3, FOV = 192 × 192 mm^2, 39 slices, TE = 25 ms, flip angle = 80 degrees. Only the 75 male samples were included in our analysis, to directly compare to our male transcriptome brain samples. In the replication datasets, all 198 individuals and 84 individuals were included as both male and female transcriptome samples are available. The preprocessing of the functional and anatomical images was done according to preprocessing scripts provided on the fcon_1000 website (http://www.nitrc.org/projects/fcon_1000). The preprocessing was done using FSL[35] and AFNI[36]. It consists of the following steps: 1. Realigning the functional images to correct for motion; 2. Spatially smoothing the functional images (Gaussian Kernel: FWHM 6 mm); 3. Rescaling the functional image to the mean; 4. Temporal band-pass filtering the functional image (0.01-0.08 Hz); 5. Removing linear and quadratic trends of the functional image; 6. Normalizing the functional image from subject space into Montreal Neurological Institute (MNI) 152 space based on T1 images using linear transformation; 7. Regressing out the global brain, white matter, CSF and motion parameter signal from the functional image. 8. Calculating mean signal time course for each region of interest (ROI). The masks for Brodmann ROIs were obtained from the software PickAltas[37] and were resampled into the same resolution as the functional images. Then frequency amplitude of low-frequency fluctuation (fALFF) was calculated as previously reported[17]. Briefly, power spectrum was computed for each ROI, the square root of which is the amplitude at each frequency. The raw fALFF index

was calculated as the sum amplitude within 0.01-0.08 Hz divided by the sum of amplitudes over the whole frequency range. For standardization purposes, the raw fALFF of each ROI was divided by the mean of the raw fALFF across all 10 ROIs. Finally, standardized fALFF was averaged across subjects to yield one value for each ROI. Then the same procedure was used to calculated fALFF in the 11 ROIs. Pearson correlation between the expression level of genes and the average fALFF among individuals were calculated. We repeated our main analysis by using Amplitude of Low Frequency Fluctuations (ALFF), another measure of resting state fMRI activity, and found that similar numbers of fMRI correlated genes are identified and their correlation levels are very similar with the fALFF results in either fMRI dataset and regardless of sex (**Supplementary Fig. 7** and **8**, respectively).

Replication datasets

The Brainspan RNA-seq data (www.brainspan.org) and Kang et al. microarray data[18] were used for gene expression replication. For each dataset, only samples from individuals aged five years or older were used. After this filtering, 378 samples from 11 neocortical regions in both left and right hemispheres in the Kang et al. dataset and 129 samples from 11 cortical regions from the Brainspan dataset were included.

Gene set enrichment analysis

Gene set enrichment analysis was performed using the PANTHER web resource to investigate the functional enrichment of genes that are positively or negatively

correlated with the fMRI signal, as measured by fALFF. We used a Bonferroni correction to control the familywise error rate at 0.05[38].

Identification of consensus gene ontology (GO) categories

To identify the consensus functional categories that are positively or negatively correlated with fMRI signal, all of the brain regions were used in the analysis. Significant GO terms were identified by PANTHER[38]. The consensus GO were defined as the GO items that are consistently significantly enriched in 2/3 gene expression datasets and in both fMRI datasets.

Identification of individual genes

To identify the individual genes with expression correlated with the fMRI signal, only the brain regions that are involved in the default mode network (DMN) were included[20]. In our RNA-seq data, 25 samples from 5 DMN regions were used (BA21, BA22, BA39, BA40 and BA9). In the Kang et al. dataset 212 samples from 6 DMN regions in both left and right hemispheres were used, and in the Brainspan dataset 72 samples from 6 DMN regions were included (IPC, OFC, MFC, ITC, STC and DFC). We considered the gene to have a reliable relationship with fALFF if the correlation exists in two of the three gene expression datasets (with two-tailed $P < 0.005$) across both of the fMRI datasets. *P* values were determined by the Fisher r-to-z transformation.

Identification of differentially expressed (DE) genes among human brain regions

Mapped reads from above were counted using HTseq-count[39] and the GRCh37 GTF provided in Ensembl release 67. Regional differentially expressed genes (genes that are differentially expressed between any brain region pair) were identified using both edgeR and DESeq in R/Bioconductor (False Discovery Rate of 0.05; Table S9 and S10)[40, 41]. Final adjusted *P* values were combined by the Fisher's combined probability test and 0.05 was used as final cutoff.

Identification of cell type specificity expression

We identified genes that preferentially are expressed in different cell types in the brain using a recently published database (http://web.stanford.edu/group/barres_lab/brain_rnaseq.html)[29] Expression levels (RPKM) of the fALFF correlated genes were obtained in different cell types to investigate the preferred expression pattern of each gene. Then the cell type that contains the greatest RPKM expression was defined as the preferentially expressed cell type (**Supplementary Table 7**). Only the fALFF-correlated genes that have expression information reported were counted and the Fisher exact test was used for the enrichment analysis of neuronal genes in the fALFF correlated genes.

Permutations to determine significance of enrichment of fALFF-correlated genes

To test whether the three gene expression datasets are correlated with the fMRI signals (fALFF) in general, large-scale permutation experiments were performed for each of them. The procedures were as follows: We calculated the number of genes correlated with fALFF (fMRI_1 and fMRI_2) in each dataset. Next, we permuted fALFF value

assignments to regions in each dataset and recalculated the correlations with fALFF (fMRI_1). We next determined the number of genes with significant correlations ($P < 0.005$) in the randomized dataset. We repeated the permutation and correlation calculations for fMRI_2 to obtain the final fALFF genes and overlapped the resultant lists from fMRI_1 and fMRI_2. Finally, we repeated these steps 1,000 times to obtain the distribution of the number of fALFF-correlated genes under the null model. A p-value was obtained by summing all the counts equal to or higher than the observed count of genes and then dividing that by the number of iterations.

Permutations to determine significance of enrichment of DE genes

To test whether differential expressed (DE) genes are more likely correlated with fALFF, permutation procedures similar to above were used except that all the DE genes were used as the background. Both DE genes from all 10 brains or only the DMN regions results in a significant p value ($P < 0.05$)**.**

Permutations to determine the co-expression of fALFF correlated genes

To test whether fALFF correlated genes have significantly higher co-expression levels than other genes, 10,000 permutations were performed. For each permutation, 38 genes were randomly sampled from the expressed gene list. Then the average co-expression values for each of them were calculated and compared with the average co-expression of the identified fALFF correlated genes. The p-value was obtained by summing all the counts equal to or higher than the observed count of co-expression and then dividing that by the number of iterations.

Statistical analysis and code availability

Pearson correlations are reported (**Figs 3a**, **b**, **c**, **d**, **supplementary Figs. 2a**, **b**, **supplementary Fig. 7, supplementary Fig. 8**). For **supplementary figure 4** and **6**, two-sided Wilcoxon rank sum tests were performed. Fisher's exact test was used to assess the significance of enrichment of fALFF correlated genes in specific cell type, DE genes and the asdM12 module. Custom scripts in R were used for all analyses and are available upon request to the corresponding authors.

References

1. Medland, S.E., Jahanshad, N., Neale, B.M. & Thompson, P.M. Whole-genome analyses of whole-brain data: working within an expanded search space. *Nat. Neurosci* **17,** 791-800 (2014).

2. Scott-Van Zeeland, A.A.*, et al.* Altered functional connectivity in frontal lobe circuits is associated with variation in the autism risk gene CNTNAP2. *Sci. Transl. Med.* **2,** 56ra80 (2010).

3. Sporns, O. Making sense of brain network data. *Nature methods* **10**, 491-493 (2013).

4. Goni, J.*, et al.* Resting-brain functional connectivity predicted by analytic measures of network communication. *Proc. Natl. Acad. Sci. USA* .**111,** 833-838 (2014).

5. Buckner, R.L. & Krienen, F.M. The evolution of distributed association networks in the human brain. *Trends Cogn. Sci.* **17,** 648-665 (2013).

6. Power, J.D.*, et al.* Functional network organization of the human brain. *Neuron* **72,** 665-678 (2011).

7. O'Connell, L.A. & Hofmann, H.A. Genes, hormones, and circuits: an integrative approach to study the evolution of social behavior. *Front. Neuroendocrinol.* **32,** 320-335 (2011).

8. Barchuk, A.R.*, et al.* Molecular determinants of caste differentiation in the highly eusocial honeybee Apis mellifera. *BMC Dev. Biol.* **7,** 70 (2007).

9. Chandrasekaran, S.*, et al.* Behavior-specific changes in transcriptional modules lead to distinct and predictable neurogenomic states. *Proc. Natl. Acad. Sci. USA* **108,** 18020-18025 (2011).

10. Geschwind, D.H. & Rakic, P. Cortical evolution: judge the brain by its cover. *Neuron* **80,** 633-647 (2013).

11. Geschwind, D.H. & Konopka, G. Neuroscience: Genes and human brain evolution. *Nature* **486,** 481-482 (2012).

12. Konopka, G.*, et al.* Human-specific transcriptional networks in the brain. *Neuron* **75,** 601-617 (2012).

13. Wang, G.Z. & Konopka, G. Decoding human gene expression signatures in the brain. *Transcription* **4,** (2013).

14. Preuss, T.M. Human brain evolution: from gene discovery to phenotype discovery. *Proc. Natl. Acad. Sci. USA* **109 Suppl 1,** 10709-10716 (2012).

15. Somel, M., Liu, X. & Khaitovich, P. Human brain evolution: transcripts, metabolites and their regulators. *Nature Rev.. Neurosci.* **14,** 112-127 (2013).

16. Biswal, B.B.*, et al.* Toward discovery science of human brain function. *Proc. Natl. Acad. Sci. USA* **107,** 4734-4739 (2010).

17. Zou, Q.H., *et al.* An improved approach to detection of amplitude of low-frequency fluctuation (ALFF) for resting-state fMRI: fractional ALFF. *J. Neurosci. Methods* **172,** 137-141 (2008).

18. Kang, H.J., *et al.* Spatio-temporal transcriptome of the human brain. *Nature* **478,** 483-489 (2011).

19. Gainetdinov, R.R., Premont, R.T., Bohn, L.M., Lefkowitz, R.J. & Caron, M.G. Desensitization of G protein-coupled receptors and neuronal functions. *Annu. Rev. Neurosci.* **27,** 107-144 (2004).

20. Buckner, R.L., Andrews-Hanna, J.R. & Schacter, D.L. The brain's default network: anatomy, function, and relevance to disease. *Ann. N. Y. Acad. Sci.* **1124,** 1-38 (2008).

21. Greicius, M.D., Krasnow, B., Reiss, A.L. & Menon, V. Functional connectivity in the resting brain: a network analysis of the default mode hypothesis. *Proc. Natl. Acad. Sci. USA* **100,** 253-258 (2003).

22. Kochubey, O. & Schneggenburger, R. Synaptotagmin increases the dynamic range of synapses by driving Ca(2)+-evoked release and by clamping a near-linear remaining Ca(2)+ sensor. *Neuron* **69,** 736-748 (2011).

23. Wallace, R.H., *et al.* Febrile seizures and generalized epilepsy associated with a mutation in the Na+-channel beta1 subunit gene SCN1B. *Nature Genet.* **19,** 366-370 (1998).

24. Marini, C., *et al.* The genetics of Dravet syndrome. *Epilepsia* **52 Suppl 2,** 24-29 (2011).

25. Fujiwara, T., *et al.* Mutations of sodium channel alpha subunit type 1 (SCN1A) in intractable childhood epilepsies with frequent generalized tonic-clonic seizures. *Brain* **126,** 531-546 (2003).

26. Carranza Rojo, D., *et al.* De novo SCN1A mutations in migrating partial seizures of infancy. *Neurology* **77,** 380-383 (2011).

27. Young-Pearse, T.L., Ivic, L., Kriegstein, A.R. & Cepko, C.L. Characterization of mice with targeted deletion of glycine receptor alpha 2. *Mol. Cell Biol.* **26,** 5728-5734 (2006).

28. Biological insights from 108 schizophrenia-associated genetic loci. *Nature* **511,** 421-427 (2014).

29. Zhang, Y., *et al.* An RNA-sequencing transcriptome and splicing database of glia, neurons, and vascular cells of the cerebral cortex. *J. Neurosci.* **34,** 11929-11947 (2014).

30. Jung, M., *et al.* Default mode network in young male adults with autism spectrum disorder: relationship with autism spectrum traits. *Mol. Autism* **5,** 35 (2014).

31. Voineagu, I., *et al.* Transcriptomic analysis of autistic brain reveals convergent molecular pathology. *Nature* **474,** 380-384 (2011).

32. Jaffe, A.E., *et al.* Developmental regulation of human cortex transcription and its clinical relevance at single base resolution. *Nat. Neurosci.* **18,** 154-161 (2015).

33. Pletikos, M., *et al.* Temporal specification and bilaterality of human neocortical topographic gene expression. *Neuron* **81,** 321-332 (2014).

34. Cioli, C., Abdi, H., Beaton, D., Burnod, Y. & Mesmoudi, S. Differences in human cortical gene expression match the temporal properties of large-scale functional networks. *PLoS One* **9,** e115913 (2014).

35. Jenkinson, M., Beckmann, C.F., Behrens, T.E., Woolrich, M.W. & Smith, S.M. Fsl. *NeuroImage* **62,** 782-790 (2012).

36. Cox, R.W. AFNI: what a long strange trip it's been. *NeuroImage* **62,** 743-747 (2012).

37. Maldjian, J.A., Laurienti, P.J., Kraft, R.A. & Burdette, J.H. An automated method for neuroanatomic and cytoarchitectonic atlas-based interrogation of fMRI data sets. *NeuroImage* **19,** 1233-1239 (2003).

38. Mi, H., Muruganujan, A., Casagrande, J.T. & Thomas, P.D. Large-scale gene function analysis with the PANTHER classification system. *Nat. Protoc.* **8,** 1551-1566 (2013).

39. Anders, S., Pyl, P.T. & Huber, W. HTSeq-a Python framework to work with high-throughput sequencing data. *Bioinformatics* **31,** 166-169 (2015).

40. Robinson, M.D., McCarthy, D.J. & Smyth, G.K. edgeR: a Bioconductor package for differential expression analysis of digital gene expression data. *Bioinformatics* **26,** 139-140 (2010).

41. Anders, S. & Huber, W. Differential expression analysis for sequence count data. *Genome Biol.* **11,** R106 (2010).

Accession codes: Gene Expression Omnibus GSE58604

Acknowledgments: This work was supported by a T32 to T.G.B. from NINDS grant T32NS048004; an NIMH grant (R00MH090238), a March of Dimes Basil O'Connor Starter Scholar Research Award, Once Upon a Time Foundation, CREW Dallas and a Jon Heighten Scholar in Autism Research Award at UT Southwestern to G.K.; the Yerkes National Primate Research Center (National Center for Research Resources P51RR165; currently Office of Research Infrastructure Programs/OD P51OD11132) to T.M.P.; and NIMH grants (5R37MH060233 and 5R01MH094714), an Autism Center for Excellence network grant (9R01MH100027), and the Simons Foundation (SFARI 206744) to D.H.G. Human tissue was obtained from the NICHD Brain and Tissue Bank for Developmental Disorders at the University of Maryland (NICHD contract numbers N01-HD-4-3368 and N01-HD-4-3383). The role of the NICHD Brain and Tissue Bank is to distribute tissue and therefore cannot endorse the studies performed or the interpretation of results.

Competing financial interests: The authors declare no competing financial interests.

Figure 1 Schematic of data analysis and results. (**a**) Significant correlations were investigated between gene expression and fMRI signal (fALFF) among different brain regions. Brodmann regions from our RNA-seq dataset are indicated in the fALFF schematic. (**b**) Three gene expression studies were utilized. The RNA-seq data in this study contained 52 left hemisphere samples in total from 10 neocortical regions, including 25 samples from 5 DMN regions; the Brainspan RNA-seq data contained 129 left hemisphere samples from 11 neocortical regions, including 72 samples from 6 DMN regions; and the Kang et al. microarray data contained 378 samples from 11 neocortical regions in both left and right hemispheres, including 212 samples from 6 DMN regions. Two resting state fMRI datasets were used, containing 198 and 84 individuals, respectively. Significantly correlated genes were identified using a Fisher r-to-z transformation, $P < 0.005$. For gene ontology all brain regions were used and for specific genes only DMN regions were used. Enrichment or significance was determined based on consistency in two out of three expression datasets.

Figure 2 Significantly more genes than expected are correlated in expression to fALFF. This indicates that this particular patterning of genes, whose expression tracks regional brain activation as measured by fALFF, is much more common than random patterns. The arrow indicates the observed number of correlated genes in each dataset ((**a**) our RNA-seq, (**b**) Kang et al., and (**c**) Brainspan). Bar plots indicate the number of correlated genes in the randomized dataset. Fold enrichment is 5, 25 and 6 for our RNA-seq, Kang et al. and Brainspan respectively. 1,000 permutations were carried out and the empirical significance level is indicated.

Figure 3 Replication of fALFF-correlated genes using two fMRI datasets. Pearson correlations between fMRI datasets using (**a**) our RNA-seq data, (**b**) Kang et al., (**c**) Brainspan and (D) an average of all three expression datasets. Red points indicate fALFF-correlated genes in only the fMRI_1 dataset. $P < 1e\text{-}10$ for all the correlations. Blue points indicate fALFF-correlated genes in only the fMRI_2 dataset. Black points indicate fALFF-correlated genes in both fMRI_1 and fMRI_2. These data demonstrate that even where genes are only correlated in one of the two fMRI datasets, the correlation levels are highly similar.

Figure 4 Expression of individual genes is correlated with fALFF signals and these correlations are greater for regional DE genes. (**a**) Heatmap view of some of the top fALFF-correlated genes. Yellow indicates smaller values in the fALFF data or gene expression and purple indicates higher values. *TP53I11*, *CCDC41, NPTXR, TNNT1, GLRA2,* and *DRD2* are negatively correlated with fALFF and *NEFH, SCN1B*, *SYT2,* and *STAC2* are positively correlated with fALFF. fALFF values from fMRI_1 are presented and the order of the normalized fALFF values is the same in both fMRI datasets. (**b**) and (**c**), Regional DE genes are more significantly correlated with fALFF than expected. Bar plots indicate DE genes correlated with fMRI. The arrow indicates the observed number of correlated DE genes. Bar plots indicate the number of correlated genes in the randomized dataset. Fold enrichment score is 8.5 for DMN regional DE genes and 11 for all 10 regional DE genes. 1,000 permutations were carried out and the empirical significance level is indicated.

Table 1 The 26 genes with expression correlated to fALFF in the same direction across datasets and >10% variation explained on average per gene.

Gene Name	Sign	Variance explained (R^2) fMRI_1			Variance explained (R^2) fMRI_2			DE gene
		In this study	Brainspan	Kang et al.	In this study	Brainspan	Kang et al.	
CCDC41	-	0.42	0.14	0.08	0.53	0.13	0.09	
NPTXR	-	0.30	0.06	0.07	0.56	0.04	0.06	Yes
TP53I11	-	0.29	0.10	0.11	0.49	0.08	0.10	Yes
PIM1	+	0.26	0.14	0.07	0.13	0.14	0.08	
DRD2	-	0.22	0.15	0.20	0.31	0.10	0.19	Yes
GLRA2	-	0.21	0.28	0.12	0.43	0.23	0.10	
NR2F2	-	0.20	0.38	0.24	0.26	0.35	0.23	Yes
NECAB2	-	0.19	0.16	0.12	0.36	0.11	0.11	Yes
PEA15	-	0.17	0.17	0.05	0.30	0.16	0.04	Yes
YPEL1	-	0.17	0.12	0.08	0.35	0.09	0.06	Yes
EPB41L4B	-	0.16	0.13	0.06	0.31	0.12	0.07	Yes
FNBP1L	-	0.14	0.16	0.06	0.30	0.15	0.05	Yes
STAC2	+	0.14	0.11	0.15	0.26	0.13	0.15	Yes
HTR2C	-	0.11	0.14	0.11	0.23	0.11	0.07	Yes
TNNT1	-	0.11	0.16	0.08	0.17	0.13	0.07	
CACHD1	-	0.10	0.12	0.09	0.24	0.13	0.08	Yes
NEFH	+	0.10	0.15	0.10	0.19	0.18	0.09	Yes
SYT2	+	0.10	0.14	0.19	0.25	0.19	0.20	Yes
KCNS1	+	0.09	0.15	0.12	0.20	0.15	0.10	Yes
SCN1B	+	0.08	0.12	0.11	0.21	0.15	0.10	Yes
SPC25	-	0.08	0.25	0.04	0.16	0.23	0.04	
RAB37	+	0.07	0.12	0.15	0.15	0.13	0.17	Yes
RAPGEF4	-	0.07	0.21	0.07	0.13	0.20	0.06	
KCTD4	-	0.06	0.18	0.19	0.19	0.16	0.17	Yes
ARHGAP6	-	0.04	0.27	0.09	0.14	0.22	0.06	Yes
GPC4	-	0.04	0.22	0.09	0.14	0.21	0.08	Yes

Supplementary Materials

Supplementary Figures 1-8

Supplementary Tables 1-10

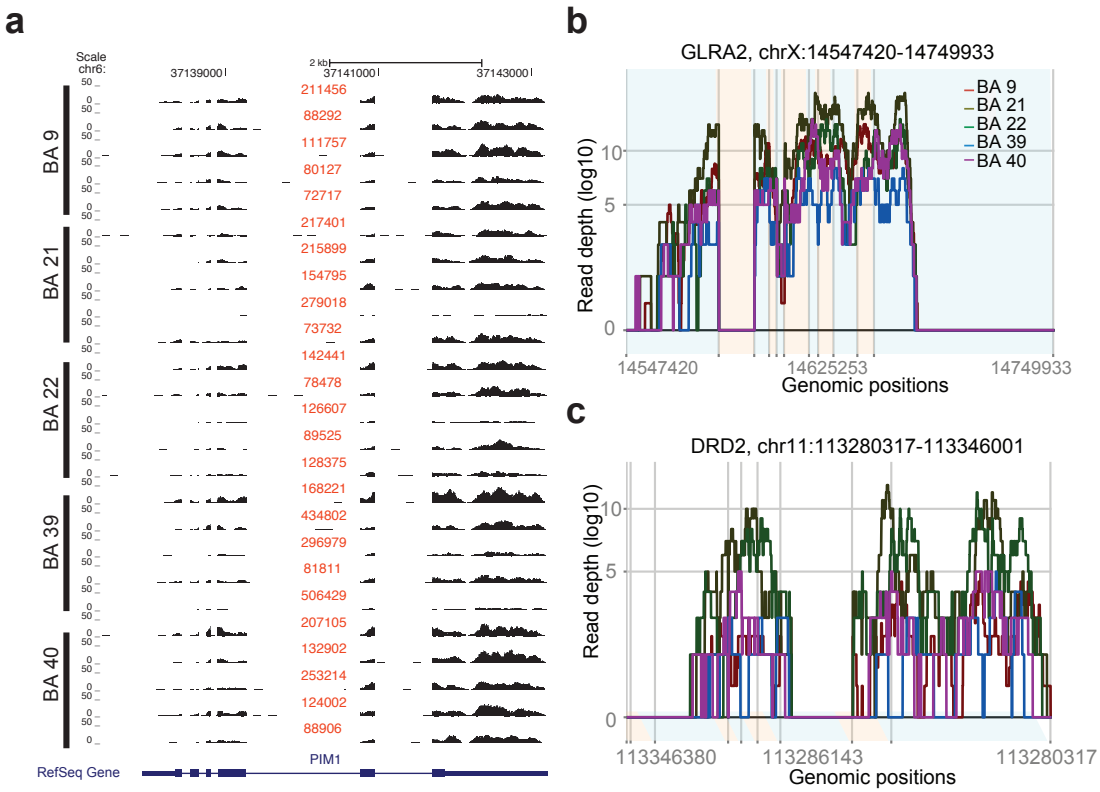

Supplementary Fig. 1 Example transcriptional profiles of genes in the DMN samples in this study. (**a**) Expression of the *PIM1* gene in five cortical areas from five individuals are displayed. RPKM values for each sample are indicated in purple text above the profile and are scaled to the same height (0-400). (**b** and **c**) Example of a non-DE gene (*GLRA2*) and a DE gene (*DRD2*). Average read depth in different cortical brain regions are shown in different colors.

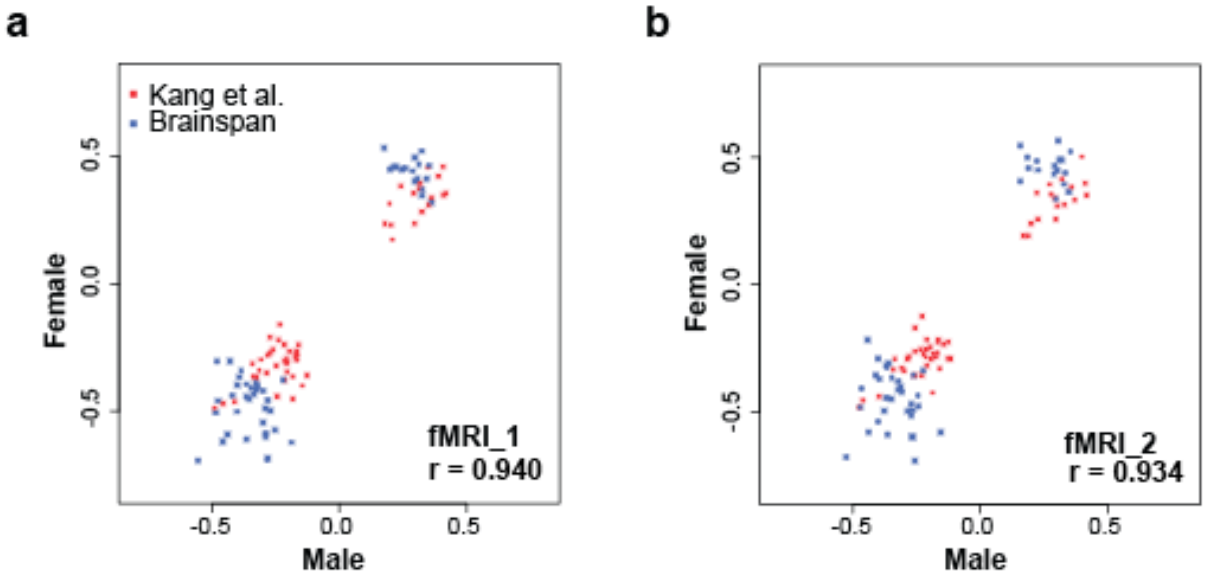

Supplementary Fig. 2 Correlation between male and female samples. Genes highly correlated with fALFF in the DMN are illustrated. *P* < 1e-10 for all the correlations. These data demonstrate that sex is not driving the observed correlations in either (**a**) fMRI_1 dataset or (**b**) fMRI_2 dataset.

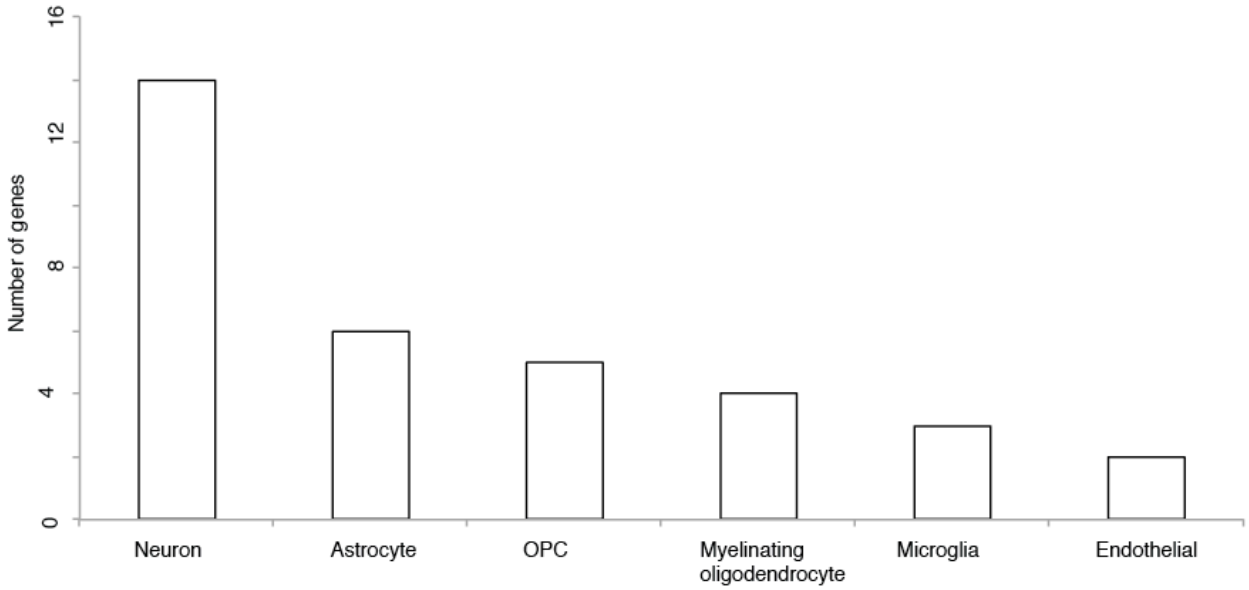

Supplementary Fig. 3 Distribution of the most fALFF-correlated genes in different brain cell types in mouse. A plurality of genes is preferentially expressed in neurons. Detailed information is described in the methods and contained in Supplementary Table 7. Data were obtained as previously reported[29].

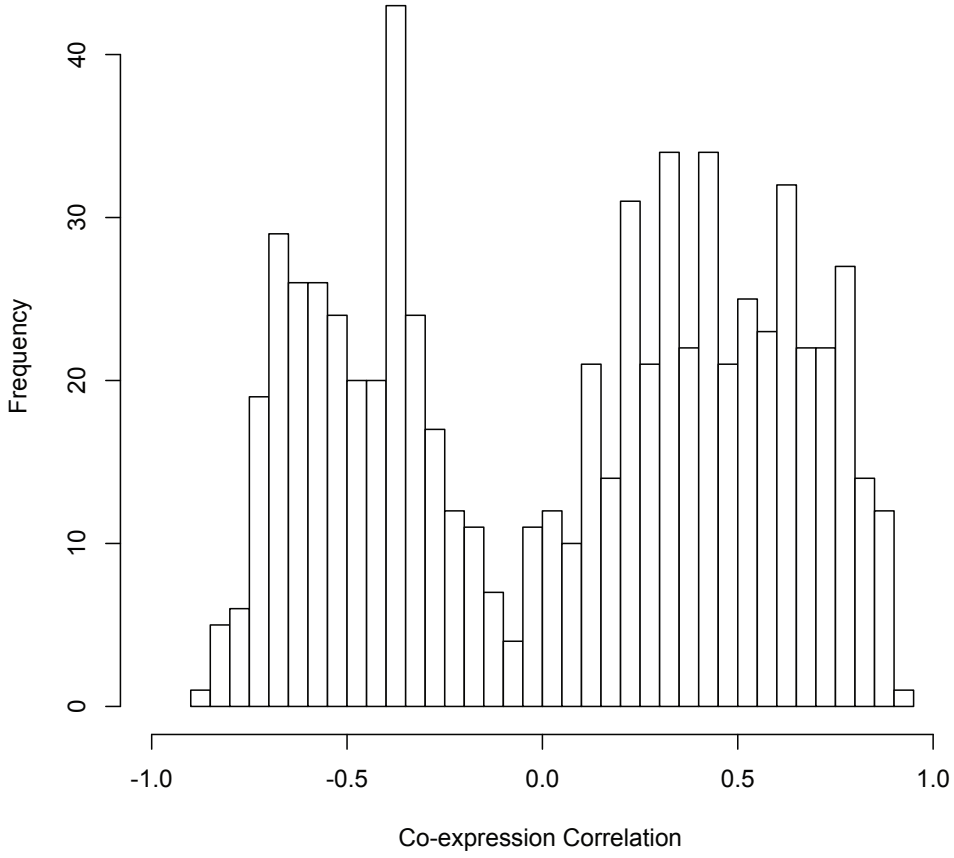

Supplementary Fig. 4 Distribution of co-expression strength of the 38 fALFF-correlated **genes.** The co-expression among the most fALFF-correlated genes is moderately correlated in both the positive and negative directions.

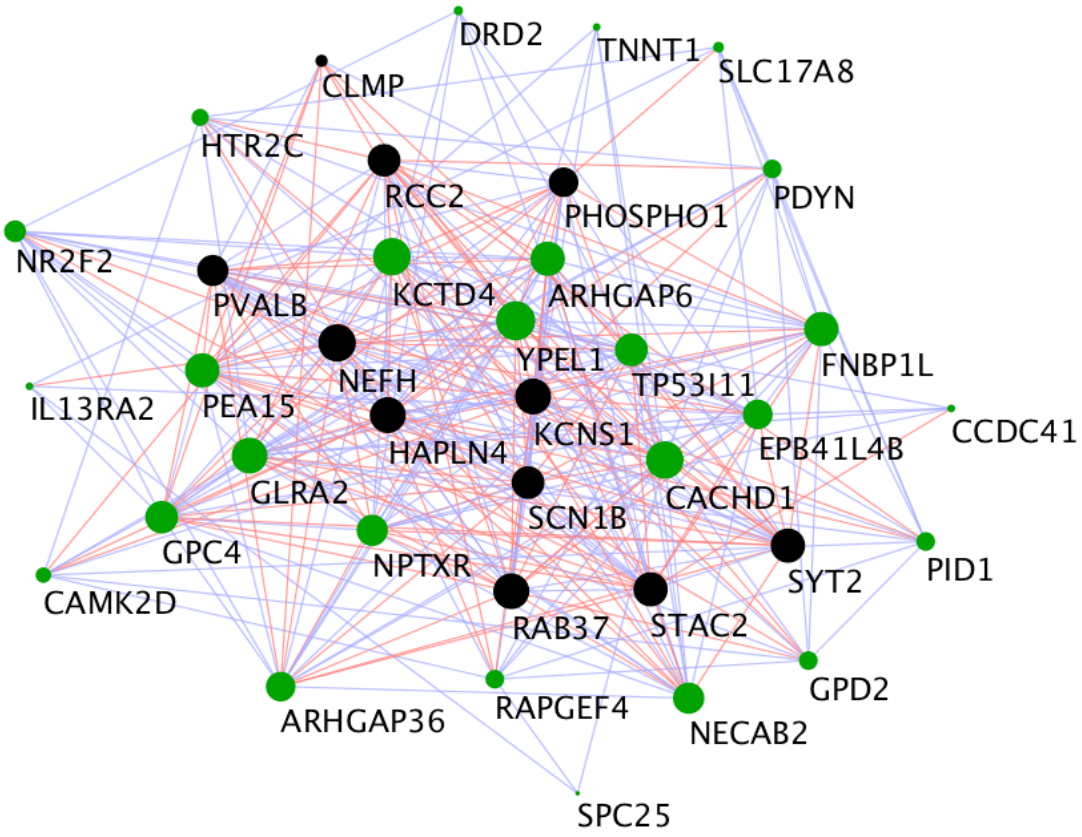

Supplementary Fig. 5 fALFF-correlated genes are highly co-expressed. Blue lines indicate negative correlations ($r < -0.5$) and red lines indicate positive correlations ($r > 0.5$). The size of the points reflects the number of connected links for a particular gene. Positively fALFF-correlated genes are highlighted in black and negatively fALFF-correlated genes are highlighted in green.

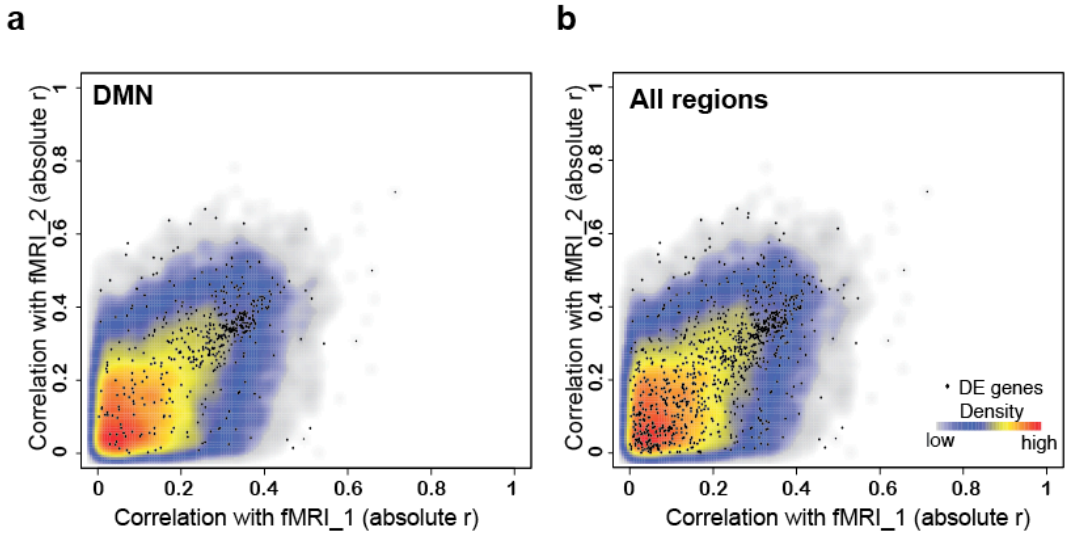

Supplementary Fig. 6 Regional DE genes are more significantly correlated with fALFF. Density plots indicating the correlation of genes between the two fMRI datasets in (**a**) only DMN regions or (**b**) all cortical brain regions. The absolute value of r is used to represent the correlation strength. Black points represent the correlation of DE genes. Other genes are plotted as a color density: grey to red indicates low to high density. $P <$ 1e-10 in all the comparisons (Wilcoxon rank sum test).

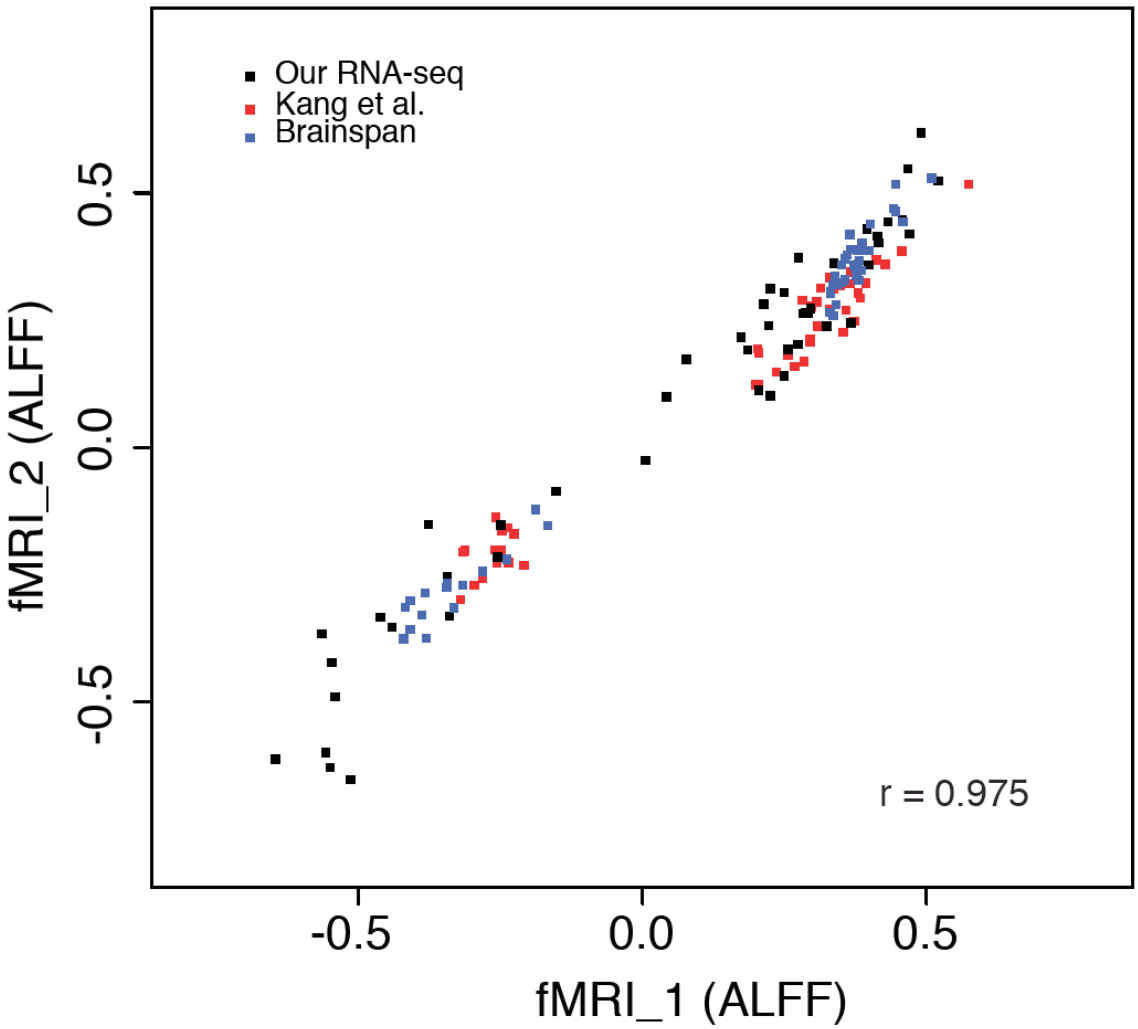

Supplementary Fig. 7 Correlation between fMRI datasets using ALFF. Using another measurement of brain activity (ALFF), we find the same high level of correlation between fMRI datasets (P < 1e-10).

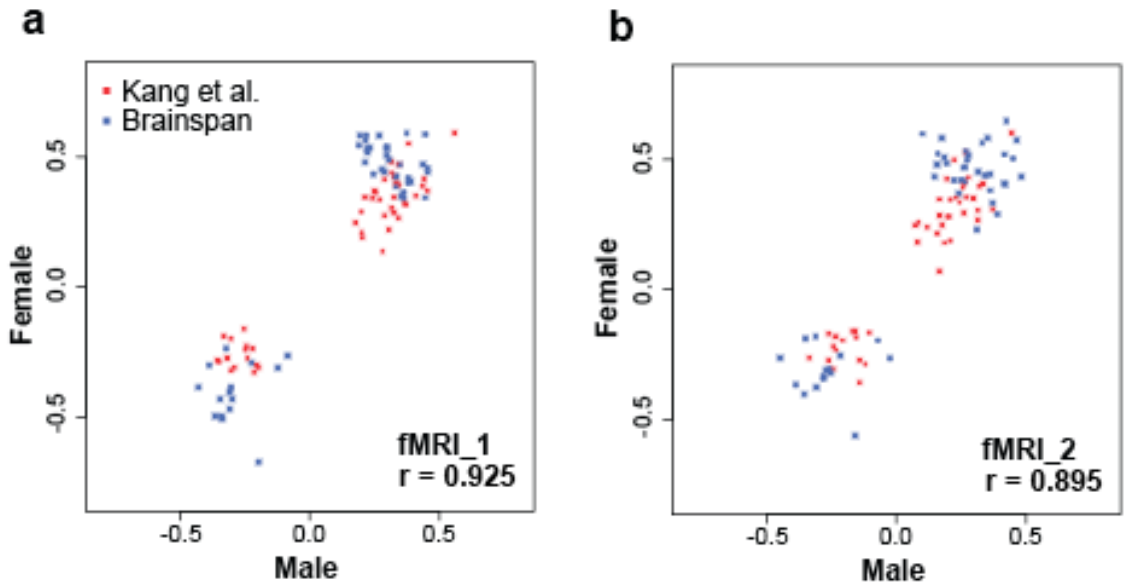

Supplementary Fig. 8 Correlation between male and female samples using ALFF. Genes highly correlated with ALFF in the DMN are illustrated and only dataset in Kang et al. and Brainspan are included as our dataset only included males. *P* < 1e-10 for all the correlations. These data demonstrate that sex is not driving the observed correlations using another measurement of brain activity, ALFF, in either fMRI_1 (**a**) or fMRI_2 (**b**) datasets.

Supplementary Table 1 Detailed information of human neocortical samples that are used in this study.

Identifier	Sex	Age	Brain Region	RIN
1029	M	30	BA21	7.0
1029	M	30	BA22	7.4
1029	M	30	BA39	6.1
1029	M	30	BA40	6.7
1029	M	30	BA44	6.2
1029	M	30	BA45	7.1
1029	M	30	BA46	6.5
1029	M	30	BA47	6.4
1029	M	30	BA6	5.5
1029	M	30	BA9	6.8
1581	M	42	BA21	3.2
1581	M	42	BA22	5.8
1581	M	42	BA39	6.0
1581	M	42	BA40	4.0
1581	M	42	BA44	6.9
1581	M	42	BA45	6.5
1581	M	42	BA46	7.3
1581	M	42	BA47	6.8
1581	M	42	BA6	4.8
1581	M	42	BA9	6.2
1905	M	33	BA21	6.6
1905	M	33	BA22	2.7
1905	M	33	BA39	4.3
1905	M	33	BA40	6.7
1905	M	33	BA44	7.8
1905	M	33	BA45	3.7
1905	M	33	BA46	8.1
1905	M	33	BA47	4.8
1905	M	33	BA6	5.6
1905	M	33	BA9	6.8
4915	M	49	BA21	7.1
4915	M	49	BA22	5.6
4915	M	49	BA39	6.9
4915	M	49	BA40	5.4
4915	M	49	BA44	6.7
4915	M	49	BA45	6.8
4915	M	49	BA46	7.7
4915	M	49	BA47	6.9
4915	M	49	BA6	7.1
4915	M	49	BA9	6.9

4924	M	48	BA21	5.2
4924	M	48	BA22	6.7
4924	M	48	BA39	5.6
4924	M	48	BA40	5.1
4924	M	48	BA44	6.5
4924	M	48	BA45	5.0
4924	M	48	BA46	5.6
4924	M	48	BA47	5.9
4924	M	48	BA6	6.5
4924	M	48	BA6	6.5
4924	M	48	BA9	6.6

Supplementary Table 2 RPKM Values.

The RPKM values can be downloaded from NCBI GEO through the following reviewer link:
http://www.ncbi.nlm.nih.gov/geo/query/acc.cgi?token=ozgnkucodnujdqt&acc=GSE58604

Supplementary Table 3 Standardized fractional Amplitude of Low Frequency Fluctuation (fALFF) for the ten brain regions in this study.

Brodmann area and hemisphere	fALFF (fMRI_1)	fALFF (fMRI_2)	Location	DMN	Abbreviation
Brodmann 21 left	0.99	0.97	Middle temporal gyrus	+	pMTG
Brodmann 22 left	0.98	0.96	Superior Temporal Gyrus	+	pSTG
Brodmann 39 left	1.05	1.06	Angular gyrus	+	AG
Brodmann 40 left	1.01	1.05	Supramarginal gyrus	+	SMG
Brodmann 44 left	0.96	0.94	Pars opercularis	_	POP
Brodmann 45 left	0.99	1.01	Pars triangularis	_	PTr
Brodmann 46 left	1.03	1.04	Middle frontal gyrus	_	MFG
Brodmann 47 left	0.99	0.96	Pars orbitalis	_	Porb
Brodmann 6 left	0.99	1.01	Pre-motor cortex	_	PMV
Brodmann 9 left	1.01	1.01	Dorsolateral prefrontal cortex	+	DLPFC

Supplementary Table 4 Standardized fractional Amplitude of Low Frequency Fluctuation (fALFF) for the brain regions in Brainspan and the Kang et al. datasets.

Abbreviation and hemisphere	fALFF (male)	fALFF (female)	fALFF (fMRI_2, male)	fALFF (fMRI_2, female)	DMN	Description
A1C left	0.94	0.93	0.90	0.94	_	Primary auditory (A1) cortex
A1C right	0.95	0.95	0.96	0.95		
DFC left	1.02	1.01	1.00	1.00	+	Dorsolateral prefrontal cortex
DFC right	1.01	1.02	0.99	1.00		
IPC left	1.04	1.01	1.03	1.01	+	Posterior inferior parietal cortex
IPC right	1.06	1.06	1.09	1.09		
ITC left	0.92	0.92	0.85	0.86	+	Inferior temporal cortex
ITC right	0.90	0.90	0.86	0.86		
M1C left	1.02	1.04	1.05	1.02	_	Primary motor (M1) cortex
M1C right	1.05	1.06	1.10	1.07		
MFC left	1.00	1.00	1.01	1.02	+	Medial prefrontal cortex
MFC right	0.99	0.98	0.97	0.98		
OFC left	0.97	0.96	0.95	0.96	+	Orbital prefrontal cortex
OFC right	0.97	0.97	0.93	0.94		
S1C left	1.03	1.05	1.11	1.07	_	Primary somatosensory (S1) cortex
S1C right	1.04	1.05	1.12	1.10		
STC left	0.98	0.98	0.95	1.02	+	Superior temporal cortex
STC right	0.98	0.99	0.98	1.01		
V1C left	1.06	1.05	1.04	1.04	-	Primary visual (V1) cortex
V1C right	1.03	1.04	1.10	1.03		
VFC left	1.04	1.02	1.04	1.05	-	Ventrolateral prefrontal cortex
VFC right	1.02	1.01	0.99	0.99		

Supplementary Table 5 Enriched consistent gene ontology items for different datasets and their significance levels.
Provided as separate .xls file

Supplementary Table 6 Detailed annotation of the 38 fALFF correlated genes.
Provided as separate .xls file

Supplementary Table 7 Cell type annotation of fALFF correlated genes. FPKM values for each cell type are indicated in the table.

Gene symbol	Astrocytes	Neuron	Oligo-dendrocyte Precursor Cell (OPC)	Newly Formed Oligodendrocyte	Myelinating Oligodendrocytes (MO)	Microglia	Endothelial Cells (EC)	Preferentially expressed cell type
Cachd1	19.1	3.9	4.9	1.6	1.1	0.1	11.3	Astrocytes
Camk2d	16.6	12.4	6.4	2.1	0.9	8.5	5.1	Astrocytes
Ccdc41	10.1	5.2	5.6	2.1	1.0	1.2	8.5	Astrocytes
Gpc4	21.5	2.3	2.9	0.2	0.2	0.1	1.4	Astrocytes
Hapln4	1.4	0.4	1.1	0.2	0.5	0.3	0.1	Astrocytes
Pdyn	4.4	1.8	0.8	0.1	0.2	0.3	0.2	Astrocytes
Gpd2	21.8	8.8	8.8	7.0	6.8	1.4	31.8	EC
Tnnt1	0.1	0.1	0.2	0.1	0.4	0.3	0.5	EC
Pim1	20.0	10.9	5.4	1.0	0.9	80.4	41.7	Microglia
Rcc2	22.4	30.9	34.6	32.4	13.0	65.8	22.5	Microglia
Scn1b	2.2	28.8	14.4	3.4	15.1	29.7	2.8	Microglia
Phospho1	0.5	0.9	1.4	2.8	12.9	1.4	2.8	MO
Pvalb	0.1	0.1	0.6	1.4	2.3	0.9	0.2	MO
Rab37	0.3	0.1	0.2	2.3	8.0	0.3	0.3	MO
Rapgef4	1.6	5.9	5.1	20.3	59.4	2.4	25.7	MO
Arhgap36	0.1	0.8	0.1	0.1	0.1	0.1	0.1	Neuron
Arhgap6	0.2	0.8	0.5	0.1	0.1	0.1	0.6	Neuron
Drd2	0.1	5.8	0.2	0.1	0.2	0.1	0.1	Neuron
Fnbp1l	11.5	54.5	14.1	2.8	0.2	1.6	24.1	Neuron
Glra2	0.1	10.4	0.1	0.1	0.1	0.1	0.1	Neuron
Htr2c	0.1	2.0	0.1	0.1	0.1	0.1	0.1	Neuron
Kcns1	0.1	0.6	0.3	0.1	0.1	0.2	0.1	Neuron
Nefh	0.1	1.4	0.3	0.1	0.3	0.2	0.1	Neuron
Nptxr	0.6	43.5	8.1	1.7	3.9	3.3	0.3	Neuron
Nr2f2	1.9	30.5	1.3	0.2	0.1	0.1	3.3	Neuron
Slc17a8	0.1	3.5	0.1	0.1	0.1	0.1	0.1	Neuron
Stac2	0.1	2.4	0.9	0.4	2.2	1.3	0.2	Neuron
Syt2	0.1	0.5	0.1	0.1	0.1	0.1	0.1	Neuron
Ypel1	0.9	11.1	5.1	2.7	1.9	1.2	1.4	Neuron
Il13ra2	0.1	0.1	0.2	0.1	0.1	0.1	0.1	OPC
Kctd4	1.7	0.9	5.7	3.0	1.9	0.1	0.2	OPC
Necab2	0.8	13.9	24.2	13.8	2.0	1.0	0.3	OPC
Pid1	12.7	9.7	60.2	12.6	0.4	5.6	1.9	OPC
Spc25	1.9	0.9	4.7	0.7	0.1	0.2	3.3	OPC

Supplementary Table 8. The 9 fALFF-correlated genes that overlap with the autism gene co-expression module, asdM12.

Ensembl ID	GeneName	Sign	Comments
ENSG00000105711	SCN1B	+	Both fMRI_1 and fMRI_2
ENSG00000100285	NEFH	+	Both fMRI_1 and fMRI_2
ENSG00000139190	VAMP1	+	Only fMRI_2
ENSG00000141750	STAC2	+	Both fMRI_1 and fMRI_2
ENSG00000177098	SCN4B	+	Only fMRI_2
ENSG00000172794	RAB37	+	Both fMRI_1 and fMRI_2
ENSG00000187664	HAPLN4	+	Both fMRI_1 and fMRI_2
ENSG00000100604	CHGA	+	Only fMRI_2
ENSG00000070159	PTPN3	-	Only fMRI_2

Supplementary Table 9 DE genes that are detected in the DMN regions. Provided as separate .xls file

Supplementary Table 10 DE genes that are detected in all 10 brain regions. Provided as separate .xls file

a

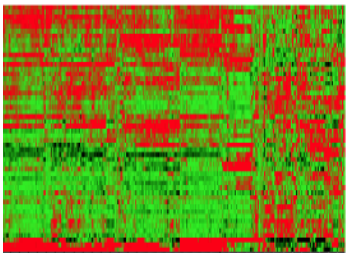

Brain gene expression

Significant correlation?

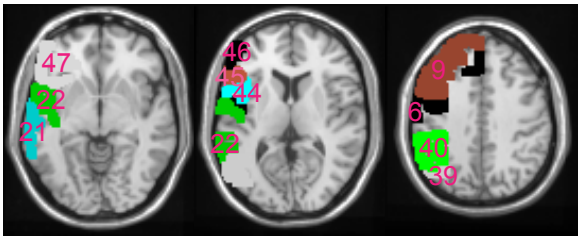

Brain functional activity (fALFF)

b

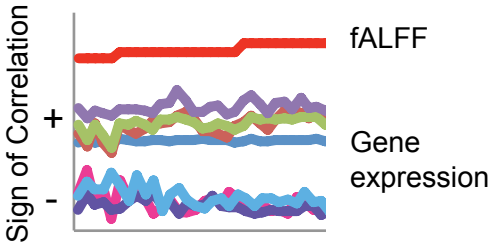

10 neocortical areas using RNA-seq in this study
11 neocortical areas using Brainspan RNA-seq
11 neocortical areas using Kang et al. microarray

&

fALFF fMRI_1
fALFF fMRI_2

All brain regions

Enrichment in 2/3 expression datasets

DMN brain regions

Significance in 2/3 expression datasets

20 functional groups enriched including:
- GPCR
- signaling receptor
- synaptic membrane

38 correlated genes ($P < 0.005$)
26 genes explain > 10% variance
Correlated to a module of co-expressed genes downregulated in postmortem ASD brains